Supporting Information

Materials and Methods

Rotation Assay. An $\alpha_3\beta_3\gamma$ mutant (α-C193S, β-His10 at amino terminus, γ-S107C, and γ–I210C) subcomplex derived from thermophilic *Bacillus* PS3 was expressed, purified, and biotinylated as described.[1] For the regeneration buffer experiments, a 0.2 nM F_1 solution in 10mM MOPS-KOH pH 7, 50 mM KCl solution (Buffer A) was infused into a microscope chamber consisting of a Ni-NTA modified bottom coverslip and an ordinary top coverslip.[2] 20 or 100 mg/ml NH_2-PEG (MW 5k, NOF Corporation, chosen by lot) in buffer A was then infused, followed by 0.29 μm streptavidin polystyrene beads (Seradyn) in Buffer A. F_1 was then pre-incubated in an 8.5 mM MOPS-KOH pH 7, 0.85 mM KCl, 110 μM $MgCl_2$ buffer (Buffer B) with 1 mM creatine phosphate (Roche), 20 μg/ml creatine kinase (Roche) and 500 nM Mg-ATP (Roche) (regeneration buffer) for 1 hour. A regeneration buffer with ~50 pM rods was then infused. For the synthesis buffer experiments the protocol was the same as previously described except no pre-incubation was performed and ~50 pM rods were injected into the chamber with 50 μM Mg-ATP, 50 μM Mg-ADP (Roche) and 50 μM sodium phosphate buffer (pH 7) in buffer B (ATP/ADP/P buffer). After incubation, a 50 Oe was briefly field applied to pin (pole) the rod magnetization. The system was then incubated in a 4.5 Oe field at 45° from the surface normal. When $|\mathbf{H}|=0$, the average angular velocity of active F_1/rod systems varied from 0.5 – 1.7 Hz. During forced rotation, $|\mathbf{H}|\sim0.5$ Oe. The rod magnetization fluctuations are negligible during the measurement.[3]

Microscopy. Rotation was observed at 23°C on an inverted microscope (IX-70 Olympus) modified with a custom built electromagnet and non-magnetic stage. Brightfield images, illuminated with a 640 nm low pass filtered halogen lamp, were acquired with Video Savant software (IO Industries) and a CCD camera (IPX-210L, Imperx) at 300 fps and 8 bit resolution. Image analysis was performed in ImageJ using centroid[4] or second moment analysis.[5]

Rod Fabrication. Rods were fabricated as described[6] with Microfab Ni 100, Preciousfab Ag4710, and Neutronex 309 Au electroplating solutions (Electroplating Engineers of Japan Ltd.) and 0.02 μm Anodisc filters (Whatman). The rods were capped with ~50 nm Au and functionalized with 10 mM biotin-dithiobis (Polypure) in a saturated propionic acid-PEG (MW 5K, NOF Corporation) ethanol solution.[7] Rod length varied from 0.7 μm – 1.8 μm as estimated from brightfield images.

Magnetic Measurement. Three sets of air coils were mounted in x, y, and z directions around a stage built of brass and aluminum and a reduced magnetization objective lens (PlanApo 100x, NA 1.4, Olympus custom-order) The field was controlled with LabVIEW software (National Instruments) and calibrated with a Hall probe (475 DSP, Lakeshore). The background magnetic field offset was nulled to < 3×10^{-3} Oe. To measure the difference in angle between θ_{ROD} and the rod's magnetization in the image plane (θ_{OFFSET}), a ~50 Oe field was applied at a known orientation, and θ_{ROD} measured. θ_{OFFSET} was typically < 20°. Repeated measurements of θ_{OFFSET} taken on the same rod but with different angles of the external field were reproducible (s.d. 3°). The rod was maintained at 45° with respect to the normal during this process.

Data Acquisition Protocol and Analysis. The majority of F_1/rod systems do not rotate in the absence of a rotating magnetic field due to adhesion of the rod to the glass surface. Very rarely, a rotating system can be found. When found, these systems often have surprisingly clean behavior. Every freely rotating system that was found was included in the analysis here.

Torque calibration using thermal fluctuation. Putting the proportionality constant (*c*) into eq. 1,

$$\tau_{EM} = c\left|\mathbf{H}_{\|}\right|\sin\left(\theta_{DIFF}\right) \qquad \text{(S1)}$$

and in the limit of small θ_{DIFF},

$$\tau_{EM} = k_{sp}\theta_{DIFF} \qquad \text{(S2)}$$

where k_{sp} is the torsional spring constant, the torque is put in simple harmonic oscillator form. This approximation allows use of the equipartition theorem

$$\tau_{EM} = \frac{k_B T}{\left\langle \theta_{DIFF}^2 - \left\langle \theta_{DIFF} \right\rangle^2 \right\rangle} \qquad \text{(S3)}$$

with k_B the Boltzmann constant, T the temperature and time average represented by angle brackets. For each F_1 system, k_{sp} was measured at nine different angles separated by 40° for 3.5 seconds with $|\mathbf{H}_{||}|$ =2.2 Oe. This resulted in a s.d. θ_{DIFF} ~7° and justified the small angle approximation. To avoid surface adhesion problems, the angle with the smallest k_{sp} (largest θ_{DIFF} variance) was used in subsequent torque calculation. This procedure gave an average torque consistent with previous measurements.[1, 8-11] The effect of camera noise on the s.d. of θ_{ROD} was negligible (<1°).

ADP Inhibition and Anomalous Rotations. To calculate the average τ_{EM}, all data were used except for rotations containing ADP inhibition events, a single anomalous synthesis rotation and slip due to weak magnetic interaction. ADP inhibition occurs when the ADP product of hydrolysis is not ejected from a binding pocket but is instead tightly held by the F_1. Hydrolysis then stops, and γ pauses 40° before the next ATP waiting angle.[12] F_1 can be mechanically reactivated by twisting the γ subunit in the hydrolysis direction and forcing the ADP out of its binding pocket, upon which F_1 resumes rotation. This reactivation requires an external torque[13] of ~ -35 pN nm (nearly equal but opposite to the mean uninhibited hydrolysis τ_{EM}). Events matching the behavior expected of reactivation from the ADP inhibited state occasionally occur during forced hydrolysis rotation (Fig. S1). The criteria we used for determining ADP inhibition is as follows. First, we define S_{run} as the average of $\sin(\theta_{DIFF})$ over a single rotation. When S_{run} is less than -0.5 times the mean S_{run} over all hydrolysis rotations of the same molecule, we say an ADP inhibition event has occurred (the -0.5 prefactor can be varied from -0.3 to -0.7 with no change in Tables 1 or S1). Out of 21 hydrolysis rotations in the regeneration buffer, 4 rotations contained an event matching this criterion. Furthermore, for all events fulfilling this criterion, the zero torque angle of the event (blue arrow in Fig. S1) which would correspond to the ADP inhibition angle is separated from the ATP binding angle by ~35° (data not shown), as is expected of ADP inhibition.[12] The

single anomalous synthesis rotation (molecule 4; Fig. S2c) may be related to a previously described type of slip[14] and is not shown in Fig. 3. Uncoupling of F_1 rotation from the magnetic field due to weak magnetic interaction (where the rod escapes the magnetic trap and performs a full hydrolysis rotation) occurred only during synthesis direction rotation in the regeneration buffer (2 rotations in molecule 1, 1 rotation in molecule 2, and multiple rotations of molecule 5) and also was not included in Fig 3.

Supporting Text

Torque Jump. The large change in θ_{DIFF} could conceivably be due to the magnetic rod suddenly pointing towards the surface normal. In this case, the magnetic interaction would decrease and θ_{DIFF} would increase. However, such phenomena would manifest as a change in the rod's appearance i.e. the rod would appear "shorter". This was checked by observing either the rod's eccentricity or the centroid of the rod as compared to the rod's center of rotation. Neither variable showed any correlation with the torque change.

ΔG_{ATP} of Regeneration Buffer Measurement. Measurements of F_1 in regeneration buffer commenced after a 1 hour incubation. Assuming all injected F_1 hydrolyze ATP at 3 ATP/sec[8, 12] in concert with the regeneration system results in a phosphate concentration of $\cong 2$ μM during F_1 measurement. As ionic strength plays little role in the phosphate potential under these conditions,[15] ADP concentration after the 1 hour incubation was calculated using Lawson et al.[16] ([ADP] $\cong$ 16 pM). These data allow the calculation of the free energy,[17] with $\Delta G_{ATP} \cong$ 22 kcal/mol estimated for this buffer condition. The relationship between ΔG_{ATP} and torque is discussed in Kinosita et al.[18]

Substrate Dependence of τ_{EM}. To verify the substrate dependence of the synthesis direction torque behaviour and to further validate the magnetic torque assay, another set of experiments were performed in a buffer containing 50 μM Mg-ADP, 50 μM Mg-ATP, and 50 μM phosphate (ATP/ADP/P buffer), which provided a ΔG_{ATP} of 13 kcal/mol. The hydrolysis torque behaviour is, once again, consistent with previous measurements (Table S1),[1, 8-11] and, as before, the synthesis direction torque is always larger than the hydrolysis direction torque (Fig. S3). However, the normalized torque ($\langle\tau_{EM}\rangle_{SYN}$ / $\langle\tau_{EM}\rangle_{HYD}$) is significantly smaller in the ATP/ADP/P buffer (1.12 ± 0.04; uncertainty is standard error of the mean) than in the regeneration buffer (1.25 ± 0.04). In many cases, the $\langle\tau_{EM}\rangle_{SYN}$ in the ATP/ADP/P buffer was only a few percent larger than $\langle\tau_{EM}\rangle_{HYD}$, in contrast to the regeneration buffer, where the smallest recorded $\langle\tau_{EM}\rangle_{SYN}$ / $\langle\tau_{EM}\rangle_{HYD}$ was 1.16. This data clearly indicates that reducing the concentrations of ADP and phosphate increases the torque required for synthesis direction rotation.

Slip in F_OF_1 ATP synthase with Low Nucleotide Concentration. A previous study on chloroplast F_OF_1 ATP synthase at low ADP concentration (less than ~10 μM) also documented a pmf related threshold for the uncoupling.[19] It was reported that the slip state was inhibited by the binding of ADP to a single catalytic site, which led to a reduced proton conduction state (increased synthesis direction torque), while the binding of a second ADP led to increased proton conduction and ATP synthesis. If such a mechanism were active in the F_1 studied here, we would expect the first synthesis direction rotation in the

regeneration buffer to have a larger average torque than the following rotations. Instead, we find the average torque of the first rotation to be less than the average torque of the remaining rotations in half of the cases. This suggests the single molecule uncoupling observed here is a different, though possibly related, phenomena to the previous study.[19]

Another study of F_OF_1 ATP synthase[14] from *Rhodobacter capsulatus* also found slip behaviour under low (< 1 μM) nucleotide concentration. Significantly, this study found no voltage threshold for slip after the onset of slip induction and is clearly different than the results of this study, which found a repeatable torque barrier to slip during consecutive slip rotations. Additionally, the *R. Capsulatus* ATP synthase study found that, once induced, slip occurs at a rate much faster than the estimated rate of proton pumping under ATP synthesis conditions (approaching that of bare F_O). In contrast, our study finds that the torque during nucleotide-deficient slip conditions is larger than the torque measured in the ATP/ADP/P buffer and therefore F_1 (in our study) rotates more slowly during slip conditions. These points show the *R. Capsulatus* F_OF_1 ATP synthase slip to be quite different from the F_1 slip of our study.

These differences in slip behaviour may be due to the differing origins of the F_1 (i.e. the F_1 by itself determines the slip behaviour) or may be related to the other subunits associated with the F_1 in the entire F_OF_1 ATP synthase complex. In both aforementioned cases of F_OF_1 ATP synthase slip,[14, 19] the origin of the slip was hypothesized to originate from the F_1 portion of the holoenzyme and not from the F_O portion. Another candidate for influencing the slip torque behaviour is the ε subunit, [20] although a previous study [21] has found little change in the angle-averaged hydrolysis torque behaviour when ε is attached to F_1.

1. Furuike, S.; Adachi, K.; Sakaki, N.; Shimo-Kon, R.; Itoh, H.; Muneyuki, E.; Yoshida, M.; Kinosita, K. *Biophysical Journal* **2008,** 95, (2), 761-770.

2. Hossain, M. D.; Furuike, S.; Maki, Y.; Adachi, K.; Ali, M. Y.; Huq, M.; Itoh, H.; Yoshida, M.; Kinosita, K. *Biophysical Journal* **2006,** 90, (11), 4195-4203.

3. Qin, J.; Nogués, J.; Mikhaylova, M.; Roig, A.; Munoz, J.; Muhammed, M. *Chem. Mater.* **2005,** 17, (7), 1829-1834.

4. Yasuda, R.; Noji, H.; Yoshida, M.; Kinosita, K.; Itoh, H. *Nature* **2001,** 410, (6831), 898-904.

5. Ballard, D. H.; Brown, C. M., *Computer Vision*. Prentice-Hall: New Jersey, 1982.

6. Reiss, B. D.; Freeman, R. G.; Walton, I. D.; Norton, S. M.; Smith, P. C.; Stonas, W. G.; Keating, C. D.; Natan, M. J. *Journal of Electroanalytical Chemistry* **2002,** 522, (1), 95-103.

7. Salem, A. K.; Searson, P. C.; Leong, K. W. *Nature Materials* **2003,** 2, (10), 668-671.

8. Sakaki, N.; Shimo-Kon, R.; Adachi, K.; Itoh, H.; Furuike, S.; Muneyuki, E.; Yoshida, M.; Kinosita, K. *Biophysical Journal* **2005,** 88, (3), 2047-2056.

9. Yasuda, R.; Noji, H.; Kinosita, K.; Yoshida, M. *Cell* **1998,** 93, 1117-1124.

10. Pänke, O.; Cherepanov, D. A.; Gumbiowski, K.; Engelbrecht, S.; Junge, W. *Biophysical Journal* **2001,** 81, (3), 1220-1233.

11. Hayashi, K.; Ueno, H.; Iino, R.; Noji, H. *Physical Review Letters* **2010,** 104, (21), 218103.

12. Hirono-Hara, Y.; Noji, H.; Nishiura, M.; Muneyuki, E.; Hara, K. Y.; Yasuda, R.; Kinosita, K.; Yoshida, M. *Proceedings of the National Academy of Sciences, USA* **2001,** 98, (24), 13649.

13. Hirono-Hara, Y.; Ishizuka, K.; Kinosita, K.; Yoshida, M.; Noji, H. *Proceedings of the National Academy of Sciences, USA* **2005,** 102, (12), 4288-4293.

14. Feniouk, B.; Mulkidjanian, A.; Junge, W. *Biochimica et Biophysica Acta (BBA)-Bioenergetics* **2005,** 1706, (1-2), 184-194.

15. Krab, K.; van Wezel, J. *Biochimica et Biophysica Acta (BBA)-Bioenergetics* **1992,** 1098, (2), 172-176.

16. Lawson, J. W.; Veech, R. L. *Journal of Biological Chemistry* **1979,** 254, (14), 6528-6537.

17. Nicholls, D. G.; Ferguson, S. J., *Bioenergetics 3*. 3rd ed.; Academic Press: 2002.

18. Kinosita, K.; Adachi, K.; Itoh, H. *Annual Review of Biophysics and Biomolecular Structure* **2004,** 33, (1), 245-268.

19. Groth, G.; Junge, W. *Biochemistry* **1993,** 32, (32), 8103-8111.

20. Feniouk, B. A.; Suzuki, T.; Yoshida, M. *Biochimica et Biophysica Acta (BBA)-Bioenergetics* **2006,** 1757, (5-6), 326-338.

21. Kato-Yamada, Y.; Noji, H.; Yasuda, R.; Kinosita, K.; Yoshida, M. *Journal of Biological Chemistry* **1998,** 273, (31), 19375-19377.

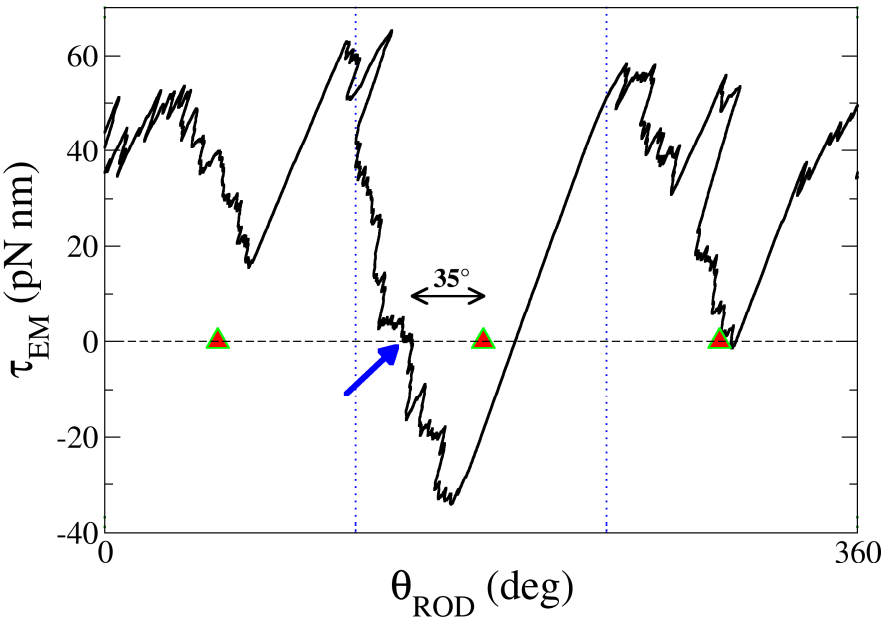

Fig. S1 | ADP inhibition. $\mathbf{H}_{||}$ rotated at 0.04 Hz in the hydrolysis direction with regeneration buffer conditions. Red triangles mark ATP waiting angles determined from the angle histogram of the same molecule released from the electromagnet. The blue arrow marks the zero torque rod angle of the ADP inhibited state. It is separated from the ATP waiting angle by 35°. Black line–100 pt. running average. Raw data not shown for clarity.

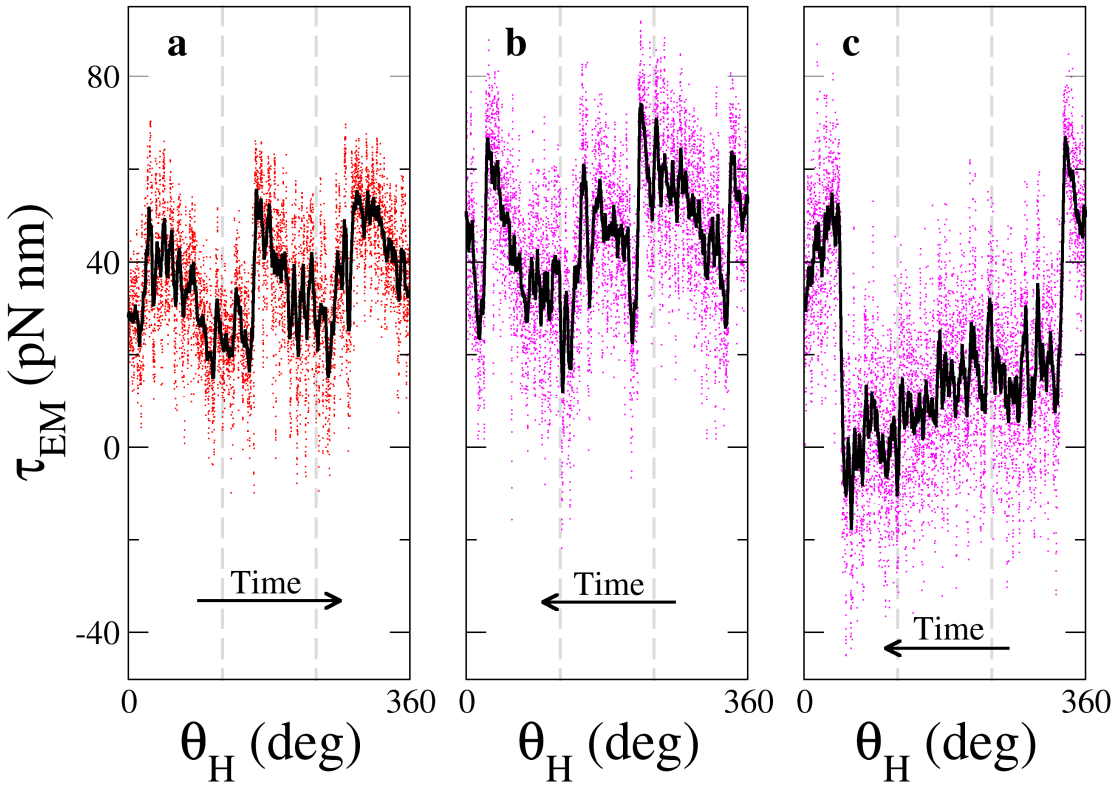

Fig. S2 | Non-reversible torque behaviour in regeneration buffer. All measurements were taken on the same F_1 with a 0.04 Hz rotating H in the hydrolysis (a) and synthesis (b and c) directions. The torque is visibly larger during synthesis rotation in most cases. The single observed exception is shown in panel c. Dots–raw data. Black line–100 pt. running average.

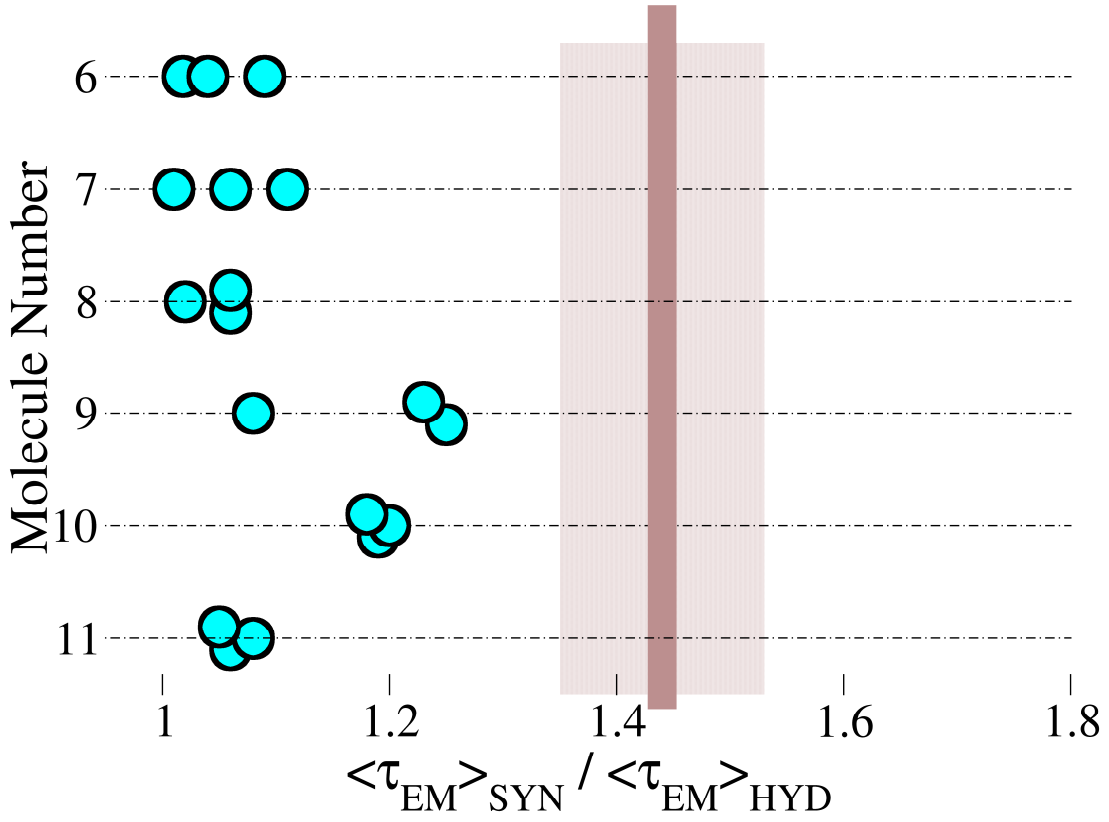

Fig. S3 | Synthesis direction rotation in ATP/ADP/P buffer. θ_H was rotated at 0.04 Hz during measurement. Each $\langle\tau_{EM}\rangle_{SYN}$ was normalized by the average $\langle\tau_{EM}\rangle_{HYD}$ for each molecule individually (taken from Table S1). The s.d. for each circular datum varied from 0.02-0.07 (not shown for clarity). Some points are offset for clarity. For comparison with Fig. 3b, the brown line once again indicates 52 pN nm, which is 130% the minimum average torque required for ATP synthesis at ΔG_{ATP} = 12 kcal/mol. To generate the normalized value, 52 pN nm is divided by the mean $\langle\tau_{EM}\rangle_{HYD}$ taken from Table S1 (s.d. due to $\langle\tau_{EM}\rangle_{HYD}$ uncertainty indicated by shaded region).

Table S1 | Average τ_{EM} in ATP/ADP/ P Buffer

Molecule No.	$<\tau_{EM}>_{HYD}$ (pN nm)	$<\tau_{EM}>_{SYN}$ (pN nm)
6	29 ± 1	30 ± 1
7	31 ± 2	33 ± 1
8	37 ± 1	39 ± 1
9	37 ± 2	48 ± 4
10	38 ± 1	45 ± 0.4
11	43 ± 2	47 ± 1
Mean	36 ± 5	40 ± 7

Results from 6 different molecules studied in ATP/ADP/P buffer. The average torque (± s.d.) over a single revolution was measured by executing 3 revolutions in the hydrolysis direction ($<\tau_{EM}>_{HYD}$) or synthesis direction ($<\tau_{EM}>_{SYN}$), excluding ADP inhibition events. θ_H was rotated at 0.04 Hz during measurement.

Movie S1

Hydrolysis rotation of F_1/rod system with rotating magnetic field in regeneration buffer. The F_1/rod is constrained from hydrolysis rotation by a magnetic field rotating at 2 mHz in the hydrolysis direction. The magnetic field orientation in the plane is indicated by the light blue circle-line symbol. ATP waiting angles are marked by filled yellow circles. The rod experiences brief "jumps" beginning at the ATP waiting angles. Playback speed 100x. Frame width = 2.48 μm.